PHYSICAL METALLURGY OF STEEL — BASIC PRINCIPLES

RN Ghosh
National Metallurgical Laboratory
Jamshedpur 831 007

INTRODUCTION

Steel is primarily an alloy of carbon in iron although most commercial grades contain other alloying elements as well. It is well known that if pure iron is slowly cooled from its liquid state to room temperature it undergoes isothermal transformations at 1534^0C from liquid to δ phase, and, at 1390^0C from δ to γ phase, and at 910^0C from γ to α phase (Fig.1). These phases have different crystal structures; δ and α phases are BCC whereas γ is FCC. Addition of carbon to iron significantly alters the above transformation characteristics. While in liquid state iron can dissolve considerable amount of carbon, its solubility in solid state is significantly less. This is determined by the spacing of iron atoms in the crystal lattice. FCC structure although more closely packed has larger interstitial spacing than BCC lattice and therefore can accommodate relatively larger amount of carbon. For example maximum solubility of carbon in α or δ (also called ferrite) is 0.08 whereas that in γ (also called austenite) it is 2.06. Carbon in excess of this limit is usually present in steel as a carbide called cementite which is a stable non equilibrium compound represented as Fe_3C. Thus steel at a given temperature and pressure may therefore contain more than one phases. Equilibrium diagram provides a graphic representation of the distribution of various phases as function temperature and overall composition. If properly interpreted this also provides compositions of respective phases and their relative amount. Fig. 2 represents such a diagram for Fe-Fe_3C system. This contains three horizontal lines representing three invariant transformations viz.

peritectic, eutectic and eutectoid; signifying coexistence of three phases of specific composition in equilibrium at a fixed temperature.

Peritectic:	L (0.55) + δ (0.08) = γ (0.18)	1493^0C
Eutectic:	L (4.30) = γ (2.06) + Fe_3C(6.67)	1147^0C
Eutectoid:	γ (0.80) = α (0.02) + Fe_3C(6.67)	723^0C

Amongst these the one which takes place completely in the solid state viz. eutectoid transformation is of considerable importance to the heat treaters. This is because solid state diffusion is relatively slow, and hence it can be completely inhibited by quenching the steel rapidly from a temperature above 723^0C giving an entirely different transformation product not indicated in the phase diagram. Development of structures ranging from equilibrium- non equilibrium constituents (or phase) in steel products forms the very basis of heat treatment technology. This lecture presents an over view of the basic principles of the evolution of various microstructures in steel and describes how it could be controlled to achieve a wide range of mechanical/physical properties the steel is known for.

Evolution of equilibrium microstructure

The progressive changes in the microstructure of a slowly cooled 0.4% C steel are illustrated schematically in Fig.3. Grains of (α) ferrite nucleates at the austenite (γ) grain boundary as the temperature drops below the point of intersection of the phase boundary with the composition line. This is called the upper critical temperature (A3). Nuclei of α grow in member as well as in size until the temperature drops to 723^0C (also called the lower critical temperature, (A1). Weight fraction of the phases can be calculated from the diagram by the lever rule, for example at 723^0C amount of austenite = (0.4 - 0.02)/(0.8 - 0.02) = 0.49.

When the alloy is cooled below 723^0C, this austenite transforms into a fine lameller structure consisting of α and Fe_3C. This is called pearlite and it has a very distinctive appearance under the microscope. Steels having ferrite-pearlite microstructure are generally called as hypoeutectoid steel. Their physical and mechanical properties are directly related to the amount of the two constituents viz. ferrite and pearlite. For example steel having 100% ferrite has a tensile strength of 40 ksi whereas the one having 100% pearlite has a strength of 120 ksi.

The behaviour of steel having more than 0.8% C is exactly similar except that there is a larger volume fraction of austenite, just above 723^0C, which subsequently transforms to pearlite, e.g., wt. fraction of austenite in 1% C is (6.67-1.0)/6.67-0.8) = 0.97; and the proeutectoid phase is Fe_3C in steel of α. The temperature at which precipitation of carbide begins in this is called Acm temperature in stead of A.

Since most commercial grades of steel contain several other alloying elements either as impurities or as intentional additions to attain specific properties, it may be worthwhile to know their effects on the equilibrium diagram of steel. Alloying additions in general brings down the carbon content of the eutectoid point; as a result % pearlite in steel having a carbon content of 0.4% for example is expected to be significantly higher 50%. In other words effective carbon content of the steel may appear to be higher than its actual value if one attempts interpret the structure in the light of the equilibrium diagram for plain carbon steel. Therefore, very often a concept of equivalent carbon is used to help interpret microstructure of alloy steel. One of the commonly used expression for carbon equivalent is as follows :

$$CE = \%C + \%\frac{Mn}{6} + \%\frac{Ni}{15} + \%\frac{Cr}{5} + \%\frac{Cu}{13} + \%\frac{Mo}{4}$$

Likewise the critical temperatures viz. A1, A3, Acm are also influenced by alloy additions. On the basis of the experimental data on a variety of steels several empirical expressions for these have been suggested. One of these is given below :

$$A1 = 723 - 10.7\ Mn - 16.9\ Ni + 29.1\ Si + 16.9\ Cr + 290\ As + 6.38\ W$$
$$A3 = 910 - 203\ \sqrt{C} - 15.2\ Ni + 44.7\ Si + 104\ V + 31.5\ Mo + 13.1\ W$$

The nature of the expressions clearly reveals that alloying elements could be broadly classified in two groups; viz. ferrite and austenite stabilizers; the former raises the austenising temperature whereas the latter lowers the same. Such expressions are extremely useful in computing appropriate austenitization temperatures for various heat treatment processes. In conjunction with the carbon equivalent concept it can help interpret microstructural evolution in slowly cooled alloy steel as well.

Non Equilibrium Microstructure

The rate of decomposition of austenite in plain carbon steel depends on how fast carbon atom diffuses through it since can not form ferrite unless local concentration of carbon drops to about 0.02 and cementite also will not form until the local carbon content builds upto 6.67. If the steel is cooled rapidly such movement can be severely restricted and altogether a totally different microstructure may evolve. Bainite and martensite are the two characteristic structures that develop in steel as a result of fast cooling. Some of their important features are given below :

Bainite may form when austenite is quenched rapidly to 200 - 400^{0}C and held there . Since the distance over which carbon atom could move at low temp. is short, a structure consisting of submicroscopic dispersion of carbides in a highly strained matrix of α evolves. Because of a finer structure and a strained matrix it has a higher strength than pearlite.

Martensite may form when austenite is quenched, to a still lower temperature. It is an extremely hard and brittle phase in which all the carbon remains in solution. Presence of excess solute in the lattice distorts the BCC structure of ferrite to body centered tetragonal (BCT). The amount of distortion expressed as c/a ratio of the unit cell is roughly proportional to the carbon content.

The transformation of austenite to pearlite and bainite as well as precipitation of proeutectoid phases occurs by a process of nucleation and growth. Such a transformation is controlled by the diffusion rate. Therefore it depends on both time and temperature. The transformation of austenite to martensite on the other hand is diffusion less and occurs so rapidly that is almost independent of time. It occurs by a shear mechanism and the fraction of γ transformed to martensite is determined by the temperature alone.

TRANSFORMATION DIAGRAM

The Fe-Fe_3C phase diagram does not represent the course which the time dependent decomposition of austenite follows. In order to represent graphically kinetics of such transformation for a given steel (say 0.8% C) it is necessary to monitor fraction of austenite that transforms to ferrite-carbide as a function of time over a range of temperatures below A1. At any given temperature such a plot has two characteristic times,

representing the start of and completion of transformation. If these two 'times' are plotted against temperature as in Fig.4 one obtains `C' shaped curves called the TTT diagram (Time-Temperature-Transformation) for that particular steel (say 0.8% C steel). The microstructures that evolve as a result of decomposition are determined by the temperature. Just below the eutectoid temperature the diffusion rate is high but the nucleation rate is low; therefore few nuclei form but they grow rapidly to produce coarse pearlitic structure with widely spaced lamellae. At temperatures couple of hundred degrees lower the nucleation rate is much higher and diffusion is slower, so a finer pearlite forms. A few hundred degrees below this bainitie is the transformation product. Martensite forms at still a lower temperature where the cooling curve intersects the *M*s - the start of the martensite transformation. If the cooling curve does not cross M_f some austenite remains untransformed.

The TTT curve exhibits a nose or minimum time before which transformation to α carbide does not begin. If martensite is to be produced, the steel must be quenched rapidly enough to avoid intersection of cooling curve with the nose. The distance of the nose from the ordinate dictates the severity of quench necessary. The purpose of adding alloying elements (except Co) is to widen this gate and thereby make it possible to produce martensite in thick sections at reasonable cooling rates and thus avoid chance of formation of surface cracks. Besides the alloy composition the size of the gate is also influenced by austenitic grain size. Coarser the grains easier it is to suppress diffusion controlled transformation and promote formation of martensite.

TTT curves of both hypo and hyper eutectoid steels have an additional curve representing the onset of the precipitation of the proeutectoid phase. A schematic diagram is shown in Fig. 5. Here as well by controlling the transformation temperature it is possible to suppress precipitation of the proeutectoid phase.

Usefulness of TTT diagrams in interpreting evolution of microstructures in steel over a range of temperatures under isothermal conditions is therefore quite obvious. However, in most heat treatment processes the job is cooled continuously except in very special cases such as austempering and martempering. Therefore it is more appropriate to construct continuous cooling transformation (CCT) diagram (Fig. 6).

Numerical procedures have also been developed to transform TTT diagram to CCT curves. However, experimental data are more dependable. CCT/TTT curves for a variety of steels are now available in the form of an atlas. Precision metallography possibly provides the most accurate estimates of such diagrams, although a majority of these may have been obtained by dilatometric studies. In certain cases hardness measurements have been used to replace metallography. Strength of various microconstituents of steel such as ferrite, pearlite and bainite are determined by their degree of fineness. For example hardness of coarser pearlite is the range of R_C 5-20 where as fine pearlite has a hardness of R_C 30-40, coarse bainite has R_C 40-45, fine bainite has R_C 50-60. Unlike these the hardness of martensite is determined primarily by its carbon content. It reaches a peak value of R_C 65 at about 0.6% carbon. This shows what a wide range of strength could be achieved in the steel only by allowing it to cool from the austenitic state at different rates e.g. R_C 5-65 (50-30ksi). Considerable efforts have been made to develop empirical regression formulas for Vickers Hardness (HV) in terms of the steel composition and cooling rate. The one popularized by Creusot Lorie are as follows :

$$HV_M = 127 + 949C + 27\,Si + 11\,Mn + 8\,Ni + 16\,Cr + 21 \log T^0$$

$$HV_B = 323 + 185\,C + 330\,Si + 153\,Mn + 65\,Ni + 144\,Cr + 191\,Mo + (89 + 53\,C - 55\,Si - 22\,Mn - 10\,Ni - 20\,Cr - 33\,Mo) \log T^0$$

$$HV_{FP} = 42 + 223\,C + 53\,Si + 30\,Mn + 13\,Ni + 7\,Cr + 19\,Mo + (10 - 19\,Si + 4\,Ni + 8\,Cr + 130\,V) \log T^0$$

when T^0 represents the mean cooling rate between 800^0C to 500^0C. Such expressions are usually valid for a class of steel. One given here is applicable for low alloy steels. However, in handbooks similar expressions are available for a variety of steels. The nature of the expressions clearly reveal whilst hardness of bainite and ferrite-pearlite structures are strong functions of cooling rate and composition, hardness of martensite is primarily determined by its carbon content. Since its coefficient is unusually high (949).

HARDENABILITY

This is a measure of the ease of forming martensitic structure in steel and is often expressed as the depth below the surface upto which such a structure develops. In a steel component or a bar of appreciable size the cooling rates at the surface and at the centre are never the same. The

difference in these rates increases with increasing severity of the cooling process. When a bar is cooled slowly in a furnace, the cooling rates at the centre and at the surface are nearly equal. On the other hand if the same bar is quenched rapidly in iced brine there is a marked difference in the cooling rates at the centre and the surface. This results in the evolution of entirely different microstructures at these two locations. Consequently the hardness profile if measured along the depth will exhibit a steep drop. Besides the material characteristics (composition and grain size) this drop in hardness depends on the section size and the severity of the quenching condition (Fig. 7). Therefore, in order to evolve a suitable measure of hardenability which is independent of size and quenching rate, the concept of ideal critical diameter designated as DI has been introduced by Grossman. This means all bars of this steel having a diameter less than DI will effectively harden throughout (i.e. it will have at least 50 martensitic structure at the centre) when cooled in an ideal quenching medium having an infinite severity of quench (H) (Fig. 8).

The Grossman method of determining DI however, is too time consuming to be of any practical application. Nevertheless it is very useful to introduce the physical concept of hardenability. A much more convenient and widely used method of determining hardenability is the Jominy End Quench test. Here a single specimen takes the place of a series of samples required in the Grossman method. The standard Jominy specimen consists of a cylindrical rod 4 inch long and 1 inch in diameter. During the test the specimen is first heated to a suitable austenitizing temperature and held there long enough to obtain a uniform austenitic structure. It is then placed in a jig and stream of water allowed to strike one end of the specimen (Fig. 9). The advantage of Jominy test is that in a single specimen one is able to obtain a range of cooling rates varying from a very rapid water quench at one end to a slow air cooling at the other. On completion of transformation of austenite, two shallow flat surfaces are ground on opposite sides of the bar and hardness test traverse is made along the length of the bar from the water quench end to the air cooled end. The data thus obtained are plotted to give Jominy hardenability curve (Fig. 10). It is seen that the hardness is the greatest where the cooling is the most rapid and Jominy. Hardenability is reported as the depth from the quenched end where the hardness value corresponds to that for 50% martensitic structure.

Considerable efforts have gone into the determination of the cooling rates at various locations on the Jominy test piece and correlating the same with cooling rates inside circular bars and other shapes. Of particular interest is the relationship between the ideal critical diameter and Jominy hardenability depth since this allows direct estimation of DI from simple Jominy tests. It is indeed because of its simplicity and a fair degree of reproducibility Jominy test has become the standard of the industry in spite of many limitations. ASTM A255-89 gives a highly specific test procedure for Jominy tests although in many instances significant deviations from the standard practice are not preventable even in most disciplined laboratories. Possibly because of this reported Jominy hardenability plots collected from various laboratories show significant scatter even for the same grade of steel (Fig. 11).

In spite of the above draw backs Jominy curves have become synonymous with hardenability of steel. Considerable efforts have been directed towards establishing a comprehensive even if relatively crude empirical expressions describing hardness distribution plots as function of composition and grain size of steel have been evolved using SAE-AISI centre line data set for a range of steel. A generalized composite formula for Rockwell C hardnesses as functions of depth (E) expressed in units of 1/16 th of an inch, valid over a range of 4/16 to 32/16 of an inch is given as

$$J_4\text{-}32 = 98\ C - 0.025\ E^2\ C + 20\ Cr + 6.4\ Ni + 19\ Mn + 34\ Mo + 28\ V + 5\ Si - 24\ \sqrt{E} + 2.86\ E - 082\ A - 1$$

whereas the quenched end hardness is given empirically as

$$J = 60\ \sqrt{C} + 20$$

where A is the ASTM grain size, E is the depth from the quenched end and the rest of the symbols denote wt% of respective alloying elements present in the steel. Some of recent studies reveal that predictions based on such expressions are often better that those arrived at by using Grossman multiplying factors for a range of steels having 0.1 to 0.6% C, 0 to 1% Si, 0 to 2% Mn, 0 to 5% Ni, 0 - 2% Cr and 0 to 0.5% (%Mo + %V). Although such relations may be valid for a limited range of composition these clearly show that hardenability improves with alloy additions and decreases with increasing austenite grain size number.

QUANTITATIVE PREDICTIONS

The concept of CCT diagram described above although helps us interpret evolution of a variety of microstructures in steel components under different cooling conditions it does not provide a direct quantitative estimate of the amount of each of the microconstituents that evolves at various locations to allow such prediction. It is necessary to represent particularly the kinetics of diffusion controlled transformation depicted on the diagram in terms of exact mathematical expressions. Subsequently connect this with the equation describing extraction of heat from the component being cooled. With the availability of fast computational facility at affordable costs. Such activities have received the attention of many research workers in the field of heat treatment technology. Amongst the currently available techniques the one suggested by Kirkaldy and his coworkers is the most comprehensive. They have used the finite element method to solve a set of coupled differential equations; one describing heat flow and the other kinetics of phase transformation; heat of reaction being the main coupling factor. This approach though most elegant takes enormously long time even on a main frame computer.

An alternative method is to solve heat transfer equations using average thermophysical properties, possibly estimated from experimental work, to compute average cooling rates at various locations and subsequently use the empirical expressions for critical cooling rates for various microstructural products to convert this into microstructures. The Creusot-Lorie procedure recommends the use of following eight critical cooling velocities Vi (in deg C/L) for different microstructures :

100% martensite :

$\log V_1 = 9.81 - 4.62C - 1.05Mn - 0.54Ni - 0.5Cr - 0.66Mo - 0.00183Pa$

90%M + 10% Bainite :

$\log V_1(10) = 8.76 - 4.04C - 0.96Mn - 0.49Ni - 0.58Cr - 0.97Mo - 0.0010Pa$

50% M + 50% B :

$\log V_1(50) = 8.50 - 4.13C - 0.86Mn - 0.57Ni - 0.41Cr - 0.94Mo - 0.0012Pa$

0% Ferrite Pearlite (smallest rate)

$\log V_2 = 10.17 - 3.80C - 1.07Mn - 0.7Ni - 0.57Cr - 1.58Mo - 0.0032Pa$

90% B + 10% FP :

$$\log V(90) = 10.55 - 3.65C - 1.08Mn - 0.77Ni - 0.61Cr - 1.49Mo - 0.0040Pa$$

50% B + 50% FP:

$$\log V_2(50) = 8.74 - 2.23C - 0.86Mn - 0.56Ni - 0.59Cr - 1.6Mo - 0.0032Pa$$

10%B + 90%FP :

$$\log V(90) = 7.51 - 1.38C - 0.35Mn - 0.93Ni - 0.11Cr - 2.31Mo - 0.0033Pa$$

100% FP (largest rate)

$$\log V_3 = 6.36 - 0.43C - 0.49Mn - 0.78Ni - 0.26Cr - 0.38Mo - 0.0019Pa - 2\sqrt{Mo}$$

where Pa (a grain growth parameter) = [1/T - (nR/Ha) log t] - 273; (where T = austenitising temperature in deg. K, t = austenitising time in hours, m = 2.303, R = 1.986 (gas constant), Ha = 110,000 cal/mole).

Using the above relationships and suitable interpolation techniques it is possible to develop a PC based computer software which could compute cooling rates at various locations of an engineering component and convert the same unto specific amount of various micro constituents present. Subsequently these could be used to estimate the hardness at various locations using the rate of mixture viz.

$$HV = (HVM \times \%M + HVB \times \%B + HV \times \%FP)/100$$

Expression for HVM, HVB and HVFP are given in equation which are valid for steels having 0.2 to 0.5% C, Si < 1%, Mn < 2%%, Ni < 4%, Cr < 3%, Mo < 1%, V < 0.2%. A range of commercial software packages based on this approach are available but these are highly component and alloy specific. Similar softwares are being developed at NML as well. Fig. 12—14 which represent a comparison of the predictive capability of the various method discussed above is an example of the output of the computer program developed at NML. We shall indeed be happy to collaborate with you to modify the same to suit your requirement.

TEMPERING

When a steel component is quenched to develop a martensitic structure residual stresses are set up. The exact nature and distribution of the stress pattern depends on the two competing processes viz. thermal contraction and volume expansion due to martensite formation. Whilst

thermal contraction induces a compressive stress at the surface, volume expansion results in a tensile stress. Strain distribution at the core is just the opposite. Exact pattern depends on the transformation characteristics of the steel determined by its composition and hardenability besides thermophysical properties, size of the component, austenitizing temperature and the severity of quench. Transformation of austenite to bainite and pearlite also produces volume expansion but of a much lesser magnitude.

Consequently quenched steels are often susceptible to cracking. Therefore, to prevent this and also to induce a fair degree of micro structural stability quenched steels are invariably subjected to a tempering process where it is heated to a temperature below A1 for a specified period. The extent of microstructural change that takes place depends on the temperature and the time, since this is a diffusion controlled process. Major microstructural changes that accompany tempering are decomposition of retained untransformed austenite to bainite or martensite and transformation of martensite into ferrite carbide aggregate. This is accompanied by a drop in strength and hardness and usually an associated improvement in ductility and toughness.

CONCLUDING REMARKS

It is impossible to cover the basic principles of heat treatment of steel within the span of one lecture. Only an attempt has been made to present a brief over view of the fundamental concepts so that you are in a position to appreciate the details which are likely to follow. Many of the points discussed here are extremely well known. These have been kept for the sake of completeness and to help understand the logic behind development of suitable quantitative structure-property prediction system for steel.

FURTHER READING

1. Metals Handbook, vol. 4, Heat Treating of Steel, ASM
2. DT Llewellyn, Steels : Metallurgy and Applications Butterworth Heinenaan, 1992
3. P.E. Readhill, Physical Metallurgy Principles, Van Nostrand Co. Inc., New York.
4. Metal progress Data Book, ASM, 1980.

5. 'End-quench Test for Hardenability of Steel' A255-89, ASTM, 1989.
6. 'Methods of Determining Hardenability of Steels', J406, Society of Automation Engineers.

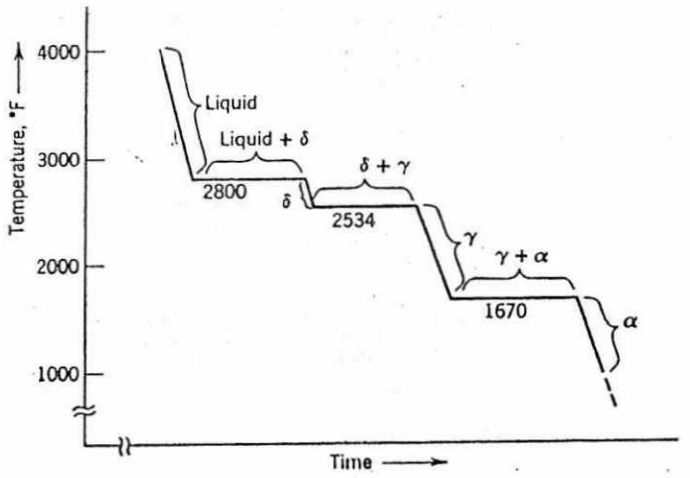

Figure 1 Schematic equilibrium cooling curve for pure iron at one atmosphere pressure.

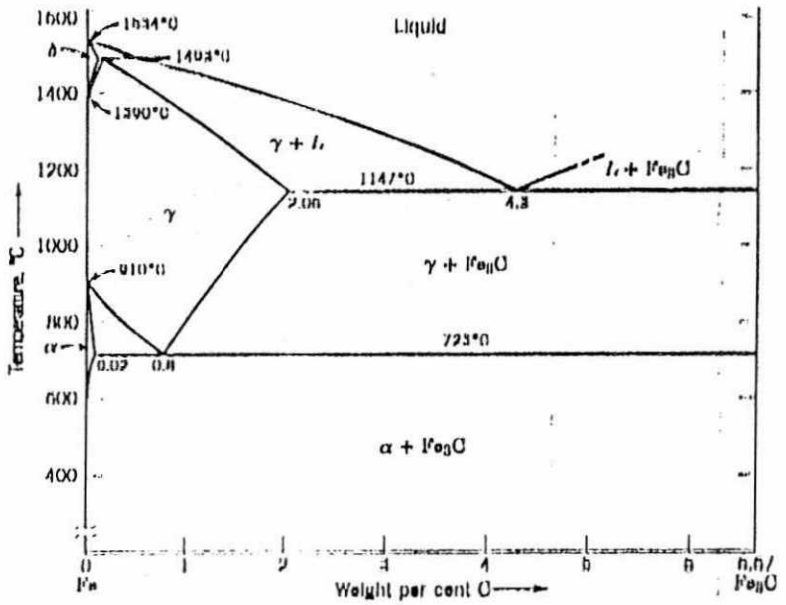

Figure 2 Phase diagram for the system Fe-Fe_3C.

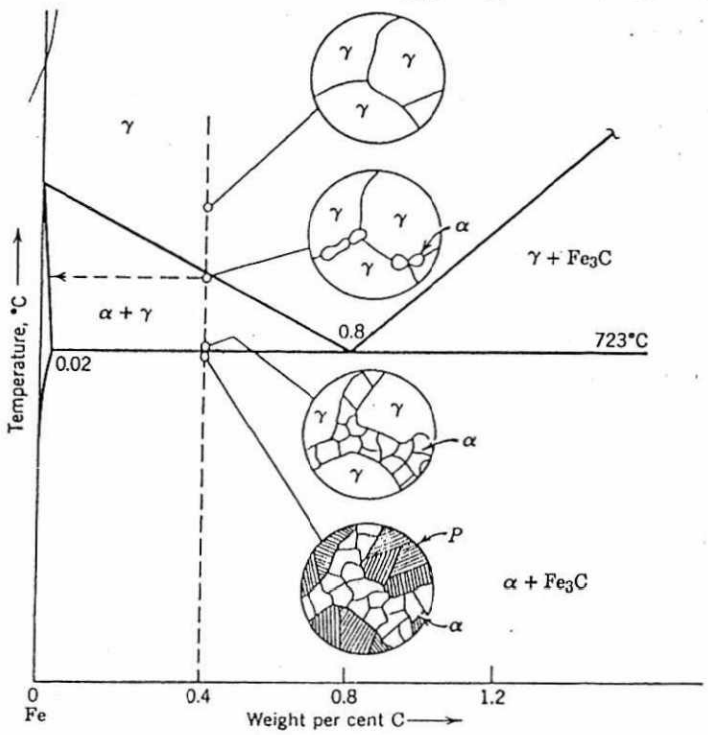

Figure 3 A schematic representation of the microstructural changes which occur during the slow cooling of a 0.4% C steel. (*a*) Austenite (γ). (*b*) Formation of α grains at γ grain boundaries. (*c*) Growth of α at grain boundaries; composition of γ is now 0.8% C. (*d*) 0.8% C γ transforms to pearlite during cooling below 723°C.

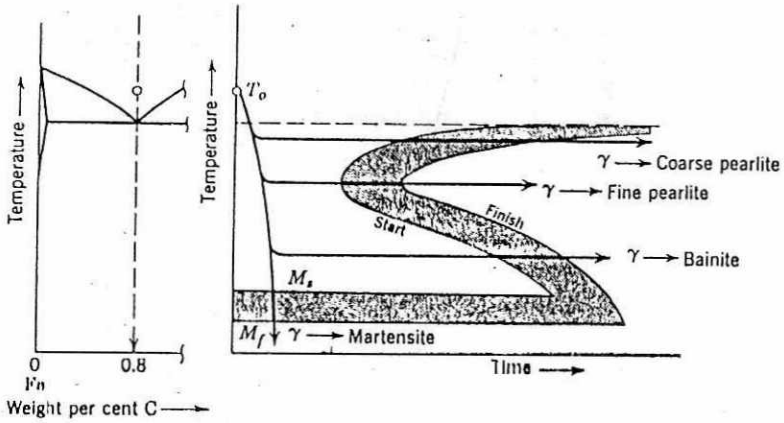

Figure 4 A *T-T-T* curve for a eutectoid plain carbon steel.

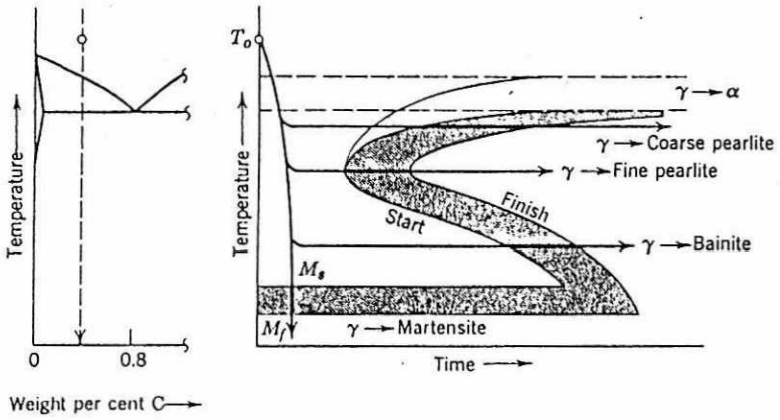

Figure 5 A *T-T-T* curve for a hypoeutectoid plain carbon steel.

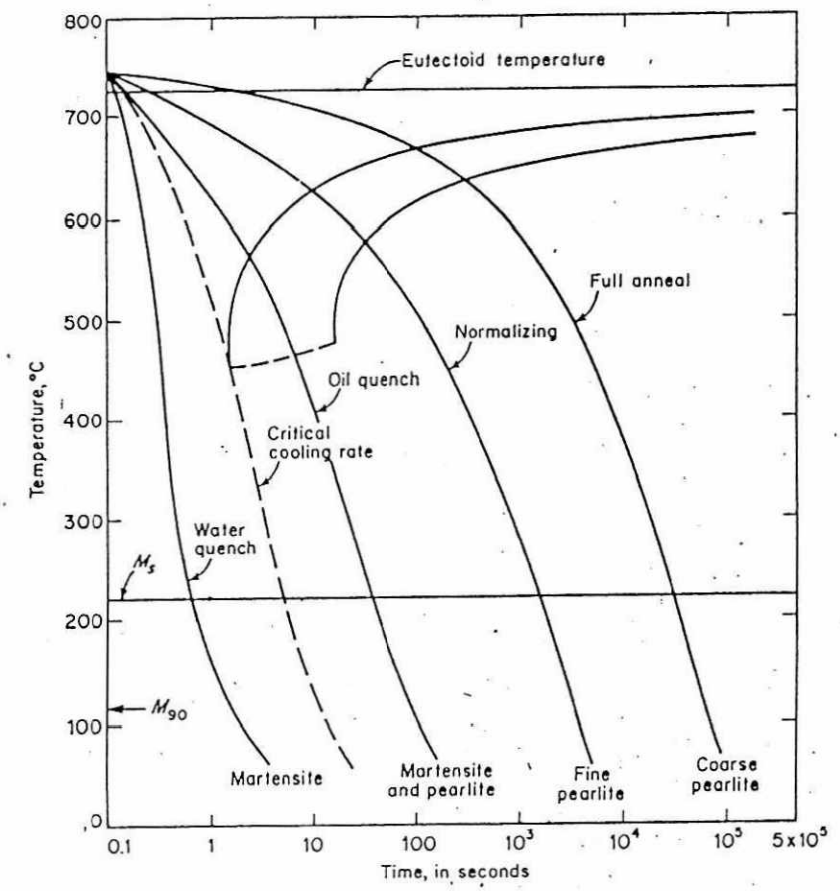

FIG. 6 The variation of microstructure as a function of cooling rate for an eutectoid steel

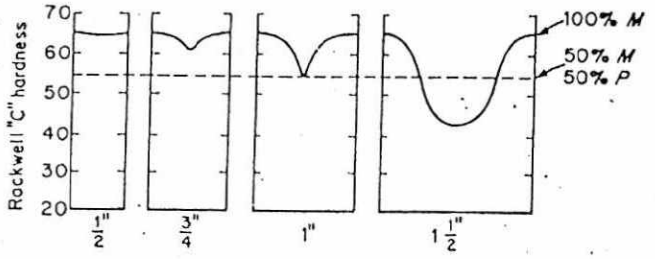

FIG. 7 Hardness test traverses similar to that of Fig. 17.4 made on a series of steel bars of the same composition, but with different diameters (schematic)

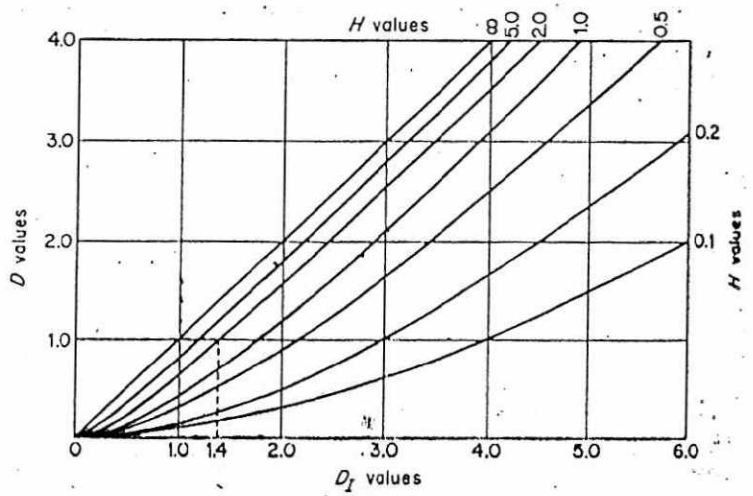

FIG. 8 Relationship of the critical diameter D to the ideal critical diameter for several rates of cooling (H values). (After Grossman, M. A., *Elements of Hardenability*, ASM, Cleveland, 1952)

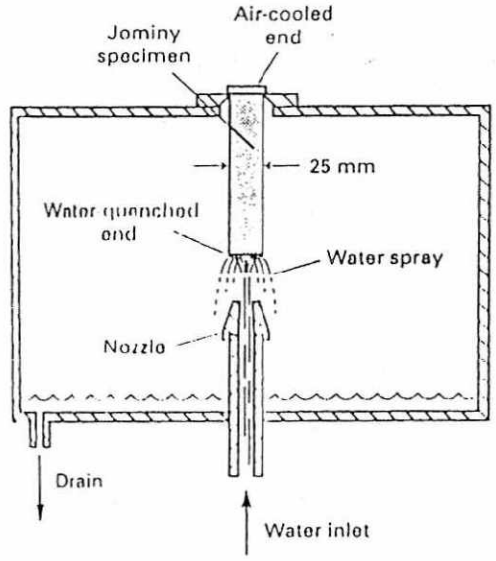

Fig 9 Hardening procedure for Jominy end-quench specimen

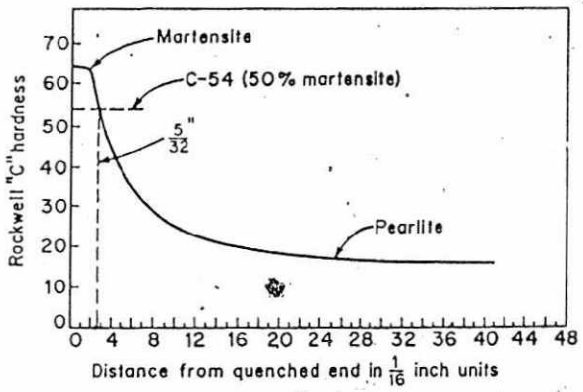

FIG. 10 Variation of hardness along a Jominy bar. (Schematic for per cent carbon)

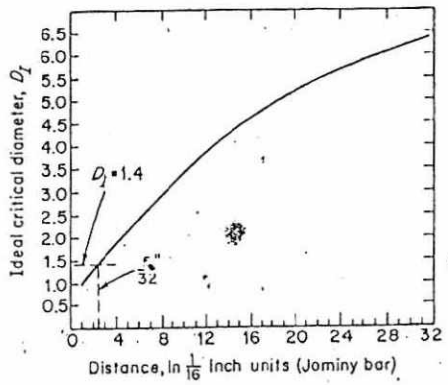

FIG. 11 Location on Jominy bar at which the cooling rate is equivalent center of a circular bar quenched in an ideal quenching medium. (After J. L., *Iron Age*, Oct. 14, 1943)

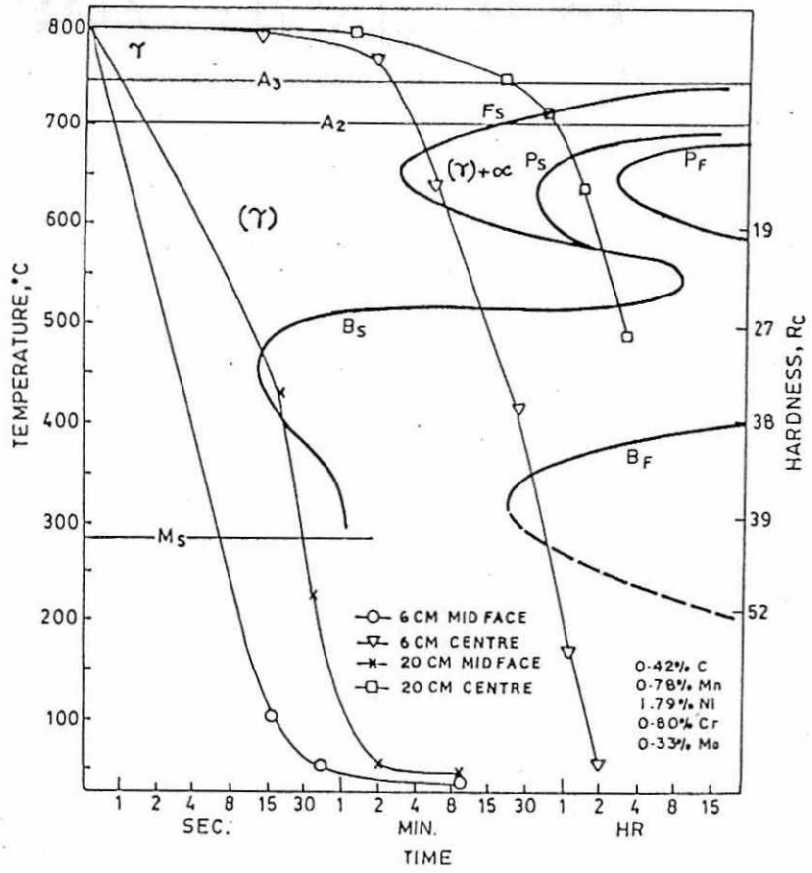

Fig. 2: Cooling curves at the surface and at the centre of 60 mm^2 and 200 mm^2 steel are superimposed on the transformation diagram for AISI 4340 steel

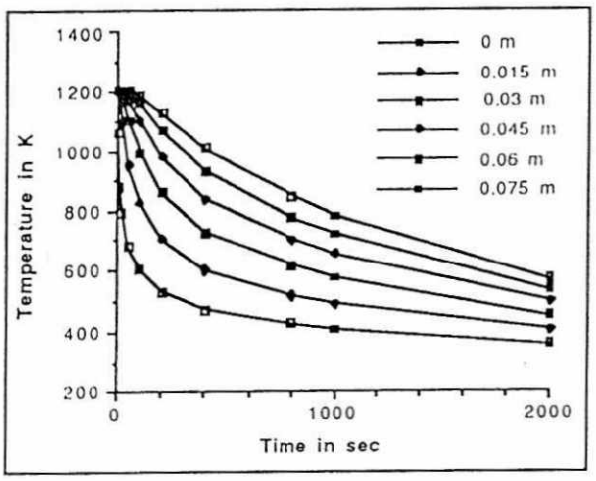

Fig. 3: Typical computed cooling curves at different locations of Jominy hardenability piece.

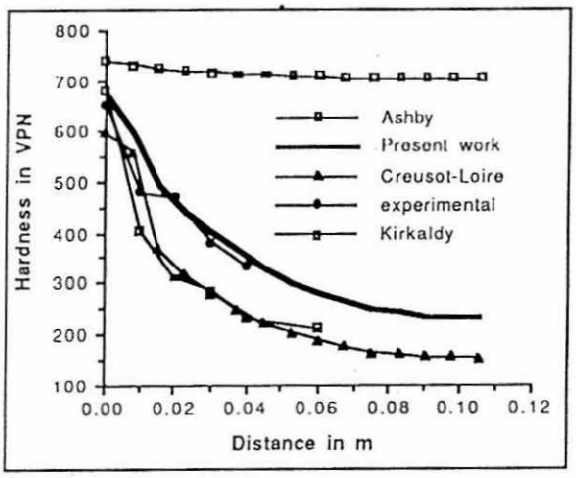

Fig. 4: A comparison of the experimental hardenability curve for AISI4140 steel with those computed using four different approaches.